Biochimica et Biophysica Acta 939 (1988) 223–237
Elsevier

BBA 73916

Membrane bilayer balance and platelet shape: morphological and biochemical responses to amphipathic compounds

James E. Ferrell Jr. *, Kathleen T. Mitchell and Wray H. Huestis

Department of Chemistry, Stanford University, Stanford, CA (U.S.A.)

(Received 6 October 1987)

Key words: Amphipath; Platelet shape; Protein phosphorylation; Membrane bilayer; (Human blood)

Activated platelets adopt a characteristic spiculate morphology. A wide variety of anionic and zwitterionic amphipathic compounds were found to effect a similar shape change and to cause the open canalicular system to become less prominent. Several cationic amphipaths reversed thrombin-, PAF-, and amphipath-induced spiculation and restored the discoid shape. Higher concentrations of cationic amphipaths caused the cells to assume spheroid and indented forms, and caused the canalicular system to appear more prominent. Three amphipaths were studied further to address possible mechanisms underlying their morphological effects. Dilauroylphosphatidylcholine was found to induce spiculation without causing the changes in protein phosphorylation and inositide metabolism generally associated with platelet activation. Two other amphipaths, chlorpromazine (which induced sphering) and dilauroylphosphatidylserine (which caused spiculation followed by sphering) caused specific changes in protein and/or lipid phosphorylation, which may be responsible for some, but not all, of the morphological effects of these compounds. To account for these findings, we propose that platelet shape can be influenced by changes in the plasma membrane bilayer balance. Agents that bind to the membrane outer monolayer are accommodated by spiculation; those that bind to the inner monolayer are accommodated by sphering.

Introduction

'Platelet activation' denotes a complex cluster of cellular phenomena that, in vivo, effect hemostasis. Activation is thought to be brought about by changes in the intracellular concentrations of one or more second messengers. For example, thrombin, collagen, ADP, and platelet activating factor (1-*O*-alkyl-2-acetyl-*sn*-glycero-3-phosphocholine, PAF), are all thought to bind to specific receptors through which they stimulate one or more inositide-specific phospholipase C's [1–3], yielding calcium mobilizing phosphoinositols [4–6] and diacylglycerol [7]. Some of the biochemical consequences of elevated calcium and diacylglycerol levels are known. Calcium stimulates calmodulin-activated myosin light chain-1 kinase [8]; one or more phospholipase A_2 activities [9], which liberate arachidonic acid (whose metabolite thromboxane A_2 is itself a platelet activator); and calcium- and aggregation-dependent proteases [10]. Diacylglycerol activates protein kinase C [7], which phosphorylates a 47 kDa protein identified by

* Present address: Department of Zoology, University of California, Berkeley, CA 94720, U.S.A.

Abbreviations: DG, diacylglycerol; DLPC, dilauroylphosphatidylcholine; DLPS, dilauroylphosphatidylserine; DMPC, dimyristoylphosphatidylcholine; IBMX, 3-isobutyl-1-methylxanthine; lysoPC, lysophosphatidylcholine; MLC1, myosin light chain 1; PAF, platelet activating factor; PI, phosphatidylinositol; PIP, phosphatidylinositol 4-phosphate; PIP_2, phosphatidylinositol 4,5-bisphosphate, PA, phosphatic acid.

Correspondence: W.H. Huestis, Department of Chemistry, Stanford University, Stanford, CA 94305, U.S.A.

Connolly et al. as inositol trisphosphate 5′-phosphomonoesterase [11]. Touqui et al. have proposed that the same kinase C substrate may be a lipocortin [12].

Together or separately, calcium and diacylglycerol can reproduce most features of platelet activation [13,14]. However, some phenomena (e.g. thrombin-induced shape changes under conditions where intracellular calcium levels are not elevated) require postulation of other intracellular signals [15]. The behavior of saponin-treated platelets is also difficult to reconcile with activation by diacylglycerol or calcium mobilization [16].

These biochemical events somehow effect a dramatic shape change, with the normally discoid platelets becoming spiculate spheres. The spicules can be fine (filopodia) or broad (pseudopodia). Shape change is generally the earliest and most easily triggered response to activators [1,2], followed by secretion and aggregation. Exceptions to this pattern include phorbol esters and synthetic diacylglycerols, which can induce secretion without concomitant spicule formation [17,18]. Spiculate platelets can recover their resting discoid shape, even after granule release has occurred [19]. Platelet shape change is accompanied by a remodeling of the cytoskeleton [20,21]. The interrelationships between activation-triggered changes in cell biochemistry, cytoskeletal organization, and membrane contour remain to be elucidated.

Under certain circumstances, human erythrocytes become spiculate in a shape change called crenation or echinocytosis. In some respects echinocytosis is similar to platelet shape change. This was first recognized by Kanaho and Fujii [22], who reported that two red cell crenators, lysophosphatidylcholine and lauric acid, cause rabbit platelets to develop fine filopodia. Two amphipaths known to cause stomatocytosis in erythrocytes (chlorpromazine and cepharanthine) caused platelets to sphere. Other cationic amphipaths are known to cause platelet sphering as well [23]. These observations, together with the observation that inositide catabolism is associated with spiculation in both erythrocytes and platelets [1–3,24–26], led us to investigate the correspondence between platelet and erythrocyte shape changes further.

In this report, we investigate the effects of a variety of previously untested amphipaths on platelet shape, and the dose-dependence and time course of these effects. We also examine the ultrastructure of amphipath-treated platelets to determine whether the open canalicular system, which is contiguous with the plasma membrane, is morphologically altered by amphipath treatment. Finally, we assess whether amphipaths might exert their morphological effects by altering inositide or protein phosphorylation.

Materials and Methods

Unless otherwise indicated, biochemicals were obtained from Sigma Chemical Company (St. Louis, MO).

Platelet isolation. Blood was obtained by venipuncture from adult volunteers who denied taking medication for the previous 14 days, and collected in silicone-coated Vacutainer tubes (Becton-Dickinson, Rutherford, NJ) containing sodium citrate to yield 10 mM. Erythrocytes and leukocytes were separated from platelet-rich plasma by centrifugation at $150 \times g$ for 15 min at room temperature. The cell pellet was reserved, and the platelet-rich plasma was recentrifuged (15 min, $150 \times g$, room temperature) to reduce erythrocyte and leukocyte contamination. Platelets were separated from plasma by gel filtration on Sepharose CL-2B [27] or by low pH centrifugation [28]. Cells were suspended in 137 mM NaCl, 2.7 mM KCl, 2 mM $MgCl_2$, 0.4 mM NaH_2PO_4, 5.6 mM glucose, 5 mM Hepes (pH 7.4); or in a similar medium buffered with 12 mM $NaHCO_3$ (pH 7.4). Gel-filtered cells were generally $(1.8 \pm 0.3) \cdot 10^8$ cells/ml. Cells isolated by centrifugation were diluted to $(1–5) \cdot 10^8$ cells/ml. In the first series of morphology experiments to be described, ADP scavengers and albumin were not included in the platelet suspension medium. Similar results were obtained in further experiments conducted in the presence of bovine serum albumin (0.1%, 'essentially fatty acid free'), apyrase (120 μg/ml), and/or phosphocreatine (700 μM) plus creatine kinase (2 U/ml). These additives were included for the protein and lipid phosphorylation experiments described below.

Erythrocyte isolation. Erythrocytes were isolated by resuspending the reserved cell pellet in 3–4 vols

of 150 mM NaCl, centrifuging at $3000 \times g$ for 5 min, and aspirating the supernatant and top layer of erythrocytes. Three saline washes were followed by one wash in 4 vols. of 138 mM NaCl, 5 mM KCl, 6.1 mM Na_2HPO_4, 1.4 mM NaH_2PO_4, 1 mM $MgSO_4$, 5 mM glucose (pH 7.4) and centrifugation at $5000 \times g$ for 10 min. Cells were resuspended in this buffer at 10% hematocrit (10^9 cells/ml).

Incubation with amphipaths. Saline suspensions (150 mM NaCl) of PAF, egg lysophosphatidylcholine (egg lysoPC), dilauroylphosphatidylcholine (DLPC, Avanti Polar Lipids, Inc., Birmingham, AL), dimyristoylphosphatidylcholine (DMPC), and dilauroylphosphatidylserine (DLPS, synthesized by D.L. Daleke using a modification of the procedure of Comfurius and Zwaal [29]) were sonicated to clarity in a bath sonicator. 1-Pyrenebutyric acid (Eastman Kodak Co., Rochester, NY) was dissolved in ethanol. Fluorescein, chlorpromazine, dibucaine, and chlorotetracycline (ICN Nutritional Biochemicals, Cleveland, OH) were dissolved in saline.

Solutions or suspensions of amphipaths were added as concentrates to suspensions of platelets or red cells in capped plastic tubes. In the case of 1-pyrenebutyric acid, the final ethanol concentration was 1% (v/v), and control cells were incubated with 1% ethanol and no amphipath. Incubations were carried out for 5 min at 37 °C in a shaking water bath, unless otherwise specified.

Thrombin activation. Platelets or erythrocytes were incubated with thrombin (0.1 to 1.0 U/ml) for 0 to 5 min at 37 °C.

Cell morphology. Aliquots of amphipath-treated and control platelets or red cells were fixed for 15 min in 1% glutaraldehyde. Platelets were examined by phase contrast microscopy with a 100 × objective. Morphology was classified as spherical (scored −1), discoid without filoposida (scored 0), discoid with one or two filopodia (scored +1), or discoid or spherical with more than two filopodia (scored +1). Erythrocytes were examined by bright field or oblique illumination with a 40 × objective and classified as discocytes (scored 0), echinocytes (scored +1 to +5, as in Ref. 30), or stomatocytes (scored −1 to −4, as in Ref. 31). The average score for a field of 100 platelets or erythrocytes was taken as the morphological index. Reproducibility of the index was approximately ± 0.15.

Samples of glutaraldehyde-fixed cells were prepared for scanning electron microscopy by washing the cells with water five times, allowing them to settle without drying on glass cover slips, freeze-drying, and sputter coating with Au-Pd. Samples for transmission electron microscopy were post-fixed in 1% OsO_4, serially dehydrated, embedded in Epon, thin sectioned, and stained with uranyl acetate and lead citrate.

To assess the number of canalicular openings per unit area on transmission electron micrographs of platelets, the following protocol was followed. Samples were coded by us, and prepared for microscopy and photographed 'single blind' (by Frances C. Thomas, Dept of Biology, Stanford University, Stanford, CA 94305). The platelet cross-sectional areas were determined by cutting and weighing photocopies of all micrographs, and the canalicular openings were counted.

Radiolabeling. Platelet-rich plasma was incubated with 1 mCi/ml $^{32}P_i$ (Amersham, carrier free) for 90 min at 37 °C. Cells were then isolated by low pH centrifugation as described above.

Lipid analysis. Phospholipids were extracted in 15 vols. of ice cold chlrooform/methanol/conc. HCl (100 : 200 : 1, v/v) plus 1 vol. 100 mM EDTA. Water (5 vols.) and chloroform (5 vols.) were added and the phases were allowed to separate. The organic phase was collected, dried under a stream of nitrogen or argon, loaded onto 2.5 × 10 cm Silica Gel HL plates (250 μm coating, Analtech, Newark, DE) and developed in chloroform/methanol/water/conc. ammonia (48 : 40 : 7 : 5, v/v). Lipid spots were stained with iodine and circled in pencil. The plates were then autoradiographed using Kodak X-OMAT AR film. Radioactive spots were scraped and quantified by liquid scintillation counting. Radiolabel in the PC spot was assumed to be constant [32] and was used as an internal standard to correct for variations in lipid loading (±15%).

Phosphoprotein analysis. Aliquots of ^{32}P-labeled platelets were added to Laemmli gel loading buffer [33], heated to 100 °C for 2 min, and subjected to SDS 12.5% polyacrylamide gel electrophoresis. In experiments not shown, 6% polyacrylamide gels were used to improve resolution of high molecular weight proteins. Gels were stained with Coomassie

blue to verify that equal amounts of protein were loaded in each lane. Stained gels were dried and autoradiographed on Kodak X-OMAT AR film at −70 °C with a Dupont Cronex screen. Gel slices were digested in 30% H_2O_2 at 60 °C overnight and their radiolabeling quantified by liquid scintillation counting.

Results

Platelets isolated by gel filtration or low pH centrifugation were irregular discs ranging from 1 to 4 μm in diameter, with zero to two fine filopodia extending from the rim of the disc (Fig. 1A). The proportions of stage 0 through +2 morphologies varied from one isolation to another, with typical morphological indices of +0.3 to +0.9 for gel-filtered platelets and +0.1 to +0.6 for cells isolated by centrifugation. The cell surface displayed openings of approx. 100 nm to the canalicular system. Prominent features of the normal platelet ultrastructure (Fig. 2a) included the plasma membrane, an underlying equatorial ring of microtubules, the extensive open canalicular system, a dense tubule system, and mitochondria and storage granules. These features have been described more extensively by others [34].

Amphiphath-induced spiculation

Platelets were treated with seven anionic or zwitterionic amphipaths: egg lysoPC micelles; DLPC, DMPC, and DLPS sonicated vesicles; and solutions of chlorotetracycline, 1-pyrenebutyric acid, and fluorescein. The morphological effects of these compounds were assessed as a function of amphipath concentration, platelet concentration, and length of incubation. All of these compounds induced cell spiculation, though on different time scales and at different concentrations (Table I; Fig. 3).

Relatively low concentrations of amphipaths produced discoid platelets with a few long, fine filopodia. At higher amphipath concentrations the number of spicules increased and the platelets became more nearly spherical. At still higher concentrations the spicules were lost and the platelets appeared as irregular spheres. This may be due to 'budding' or vesiculation of the filopodia [35]. Spiculate platelets produced by amphipath treatment were morphologically indistinguishable from

TABLE I

THE EFFECTS OF AMPHIPATHS ON PLATELET AND ERYTHROCYTE SHAPE

Platelets ($(1.7 \pm 0.2) \cdot 10^8$ cells/ml) and erythrocytes (10^9 cells/ml) were incubated with amphipaths for 5 min at 37 °C (2 h for DMPC), and their morphologies assessed.

Compound	Platelets		Erythrocytes	
	effect on shape	half maximal concentration (μM)	effect on shape	half maximal concentration (μM)
PAF	spiculation	1.5 ± 0.5	echinocytosis	7 ± 2
DLPC	spiculation	2 ± 1	echinocytosis	7 ± 2
Egg lysoPC	spiculation	5 ± 1	echinocytosis	10 ± 2
DMPC	spiculation	15 ± 2	echinocytosis	10 ± 2
1-Pyrenebutyric acid	spiculation	45 ± 15	echinocytosis	180 ± 60
Fluorescein	spiculation	4500 ± 500	echinocytosis	5000 ± 1000
DLPS	biphasic	5–20	biphasic	20–50 [a]
Chlorpromazine	sphering	20 ± 10	stomatocytosis	110 ± 30
Dibucaine	sphering	n.d. (< 150)	stomatocytosis	600 ± 100
Tetracaine	sphering	n.d. (< 150)	stomatocytosis	n.d.
Theophylline	none	> 3000	none	> 3000
3-Isobutyl-1-methylxanthine	none	> 900	none	> 900

[a] Estimated from Ref. 17 and D.L. Daleke, personal communication.

cells activated by PAF (100 nM), ADP (50 μM), or collagen (10 μg/ml). Thrombin-stimulated platelets were similar in appearance but their spicules tended to be shorter and broader (pseudopodia).

The ultrastructure of a spiculate, DLPC-treated platelet is shown in Fig. 2b. This micrograph shows numerous filopodia roughly 100 nm in diameter, some containing longitudinally arrayed microtubules. Peripheral microtubules are also

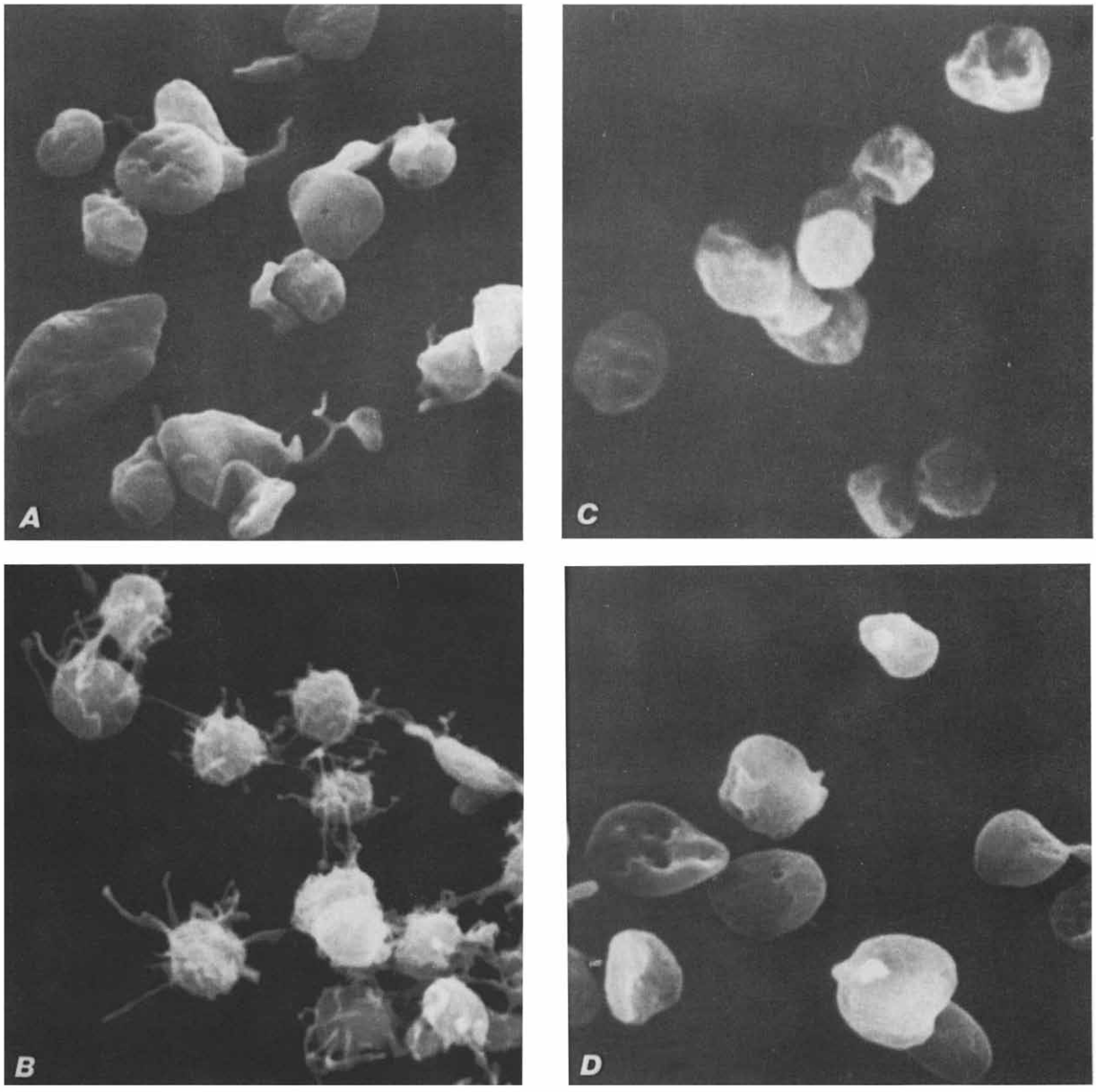

Fig. 1. Scanning electron micrographs of control and amphipath-treated platelets. (A) Untreated platelets, discoid with few filopodia. (B) Spiculate platelets, produced by incubating cells ($1.8 \cdot 10^8$/ml) with egg lysoPC (25 μM). (C) Spheroid and indented platelets produced by incubating cells ($1.8 \cdot 10^8$) with chlorpromazine (50 μM). (D) Discoid platelets produced by incubating cells ($1.8 \cdot 10^8$/ml) with egg lysoPC (25 μM), followed by addition of chlorpromazine (50 μM). Magnification: 8500×.

seen just inside the cell body. No 'internal contraction' [34] is apparent. The open canalicular system is less prominent in spiculate platelets than in untreated platelets; from this and other micrographs, the number of canalicular openings per unit cross-sectional area decreased about 2-fold.

The most potent amphipath, DLPC, was at least 20-fold less potent than the structurally related compound PAF. DLPC-induced spiculation was half-maximal at a concentration of roughly $6 \cdot 10^6$ molecules per cell. The amounts of DLPC, DMPC, or egg lysoPC required to produce half-maximal spiculation varied approximately linearly with platelet concentration over a range of $(1-5) \cdot 10^8$ platelets/ml.

Half-times for amphipath-induced spiculation

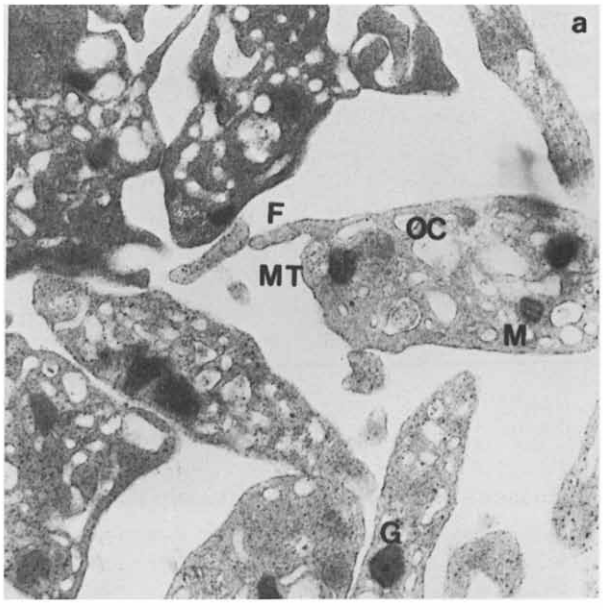

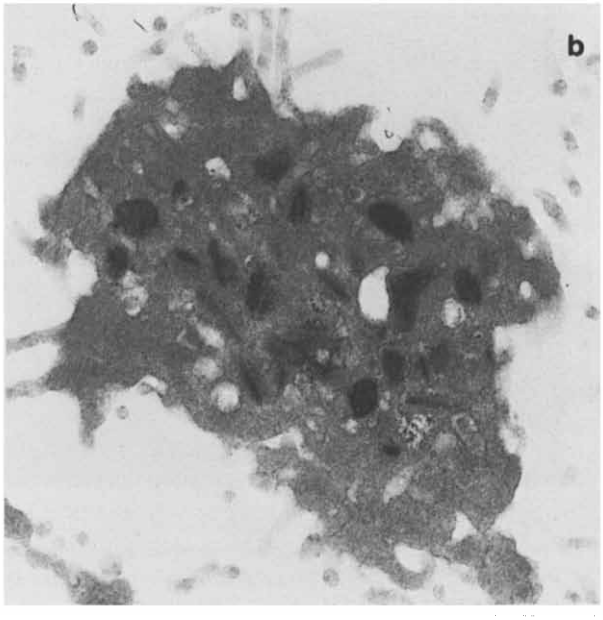

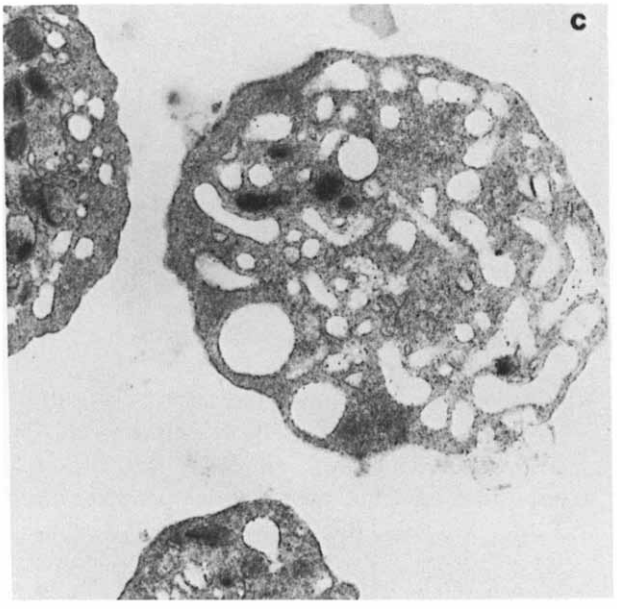

Fig. 2. Transmission electron micrographs of control and amphipath-treated platelets. (a) Untreated platelets. Shown are F, filopodium; G, granule; M, mitochondrion; MT, circumferential band of microtubules; OC, open canalicular system. (b) DLPC-treated platelets. Cells ($5 \cdot 10^8$/ml) were incubated with DLPC (40 μM) for 5 min at 37 °C. (c) DLPC- and chlorpromazine-treated platelets. Cells were incubated for 5 min and DLPC as in (b) followed by 140 μM chlorpromazine for 5 min. Magnification: 17500×.

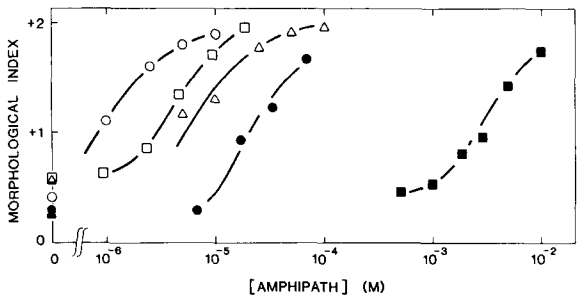

Fig. 3. Dose-response curves for platelets ($1.8 \cdot 10^8$/ml) incubated with amphipaths. ○, DLPC; □, egg lysoPC; △, DMPC; ●, 1-pyrenebutyric acid; ■, fluorescein.

ranged from less than 30 s for egg lysoPC to 1 ± 1 min for DLPC and 45 ± 15 min for DMPC. These time scales are consistent with the reported rates of intermembrane transfer for the respective lipids [36]. DLPC- and egg lysoPC-treated cells remained spiculate for at least 30 min. DMPC-treated cells remained spiculate for at least 1 h.

DLPS-induced biphasic shape change

As previously reported [31], the effects of DLPS on platelet shape were more complex. At concentrations of 10–25 μM (platelet concentration $2 \cdot 10^8$ cells/ml), DLPS induced rapid spiculation with a half-time of roughly 2.5 min. This spiculation was followed by recovery of the discoid form and then by sphering (Fig. 6); occasional indented forms were also seen (vide infra). Lower concentrations effected sphering without the transient spiculation.

Amphipath-induced sphering

Platelets were treated with three cationic amphipaths: chlorpromazine, dibucaine, and tetracaine. At low concentrations, these agents caused the few spicules found in untreated platelets to disappear. Treated with higher amphipath concentrations, the platelets became more nearly spherical and developed surface irregularities and occasional indentations (Fig. 1C). A few such platelets displayed large invaginations (Fig. 4C), which might be exaggerated openings of the canalicular system.

Compensatory shape changes

Platelets were treated with egg lysoPC or DLPC at concentrations sufficient to cause marked spiculation. The spiculate cells were then treated with chlorpromazine, dibucaine, or tetracaine. Subsequently, they regained discoid form, and finally became spherical and indented (Fig. 1D). The discoid PC-plus-chlorpromazine treated platelets were indistinguishable from untreated (resting) platelets, and the spheroid platelets were indistinguishable from cells treated with chlorpromazine alone. Spheroid DLPS-plus-chlorpromazine-treated platelets appeared to possess a more extensive (2–3-fold more openings per unit cross sectional area) and more dilated open canalicular system than did untreated platelets (Fig. 2c and other micrographs not shown). Alternatively, some of these dilated openings might represent empty secretory granules.

Chlorpromazine and dibucaine also reversed the morphological effects of thrombin and PAF (Fig. 5a), again with a half time of roughly 2.5 min. Similar concentrations of amphipaths were required to reverse the effects of physiological platelet agonists (25–50 μM chlorpromazine per $2 \cdot 10^8$ thrombin- or PAF-activated cells). Conversely, egg lysoPC reversed the morphological effects of chlorpromazine (30 μM) (Fig. 5b). At higher chlorpromazine concentrations, egg lysoPC only partially reversed the effects of chlorpromazine.

Inhibitors

Albumin (possibly a prostaglandin scavenger [1]) and an ADP scavenger (either apyrase or creatine kinase plus phosphocratine) are often added to platelet suspensions as 'stabilizers'. Platelets were incubated with DLPC, DLPS, or chlorpromazine in the presence of these agents. As in their absence, DLPC caused spiculation, and DLPS caused transient spiculation followed by sphering (data not shown). Aspirin treatment either in vivo or in vitro had no effect on egg lysoPC-induced spiculation. Thus the shape change does not require either ADP or thromboxane release.

Agents that elevate platelet cAMP tend to render the cells resistant to activation, perhaps by accelerating the removal of calcium from the cytoplasm [37]. Since many cationic amphipaths, including chlorpromazine, dibucaine, and tetracaine, are known calmodulin inhibitors and some

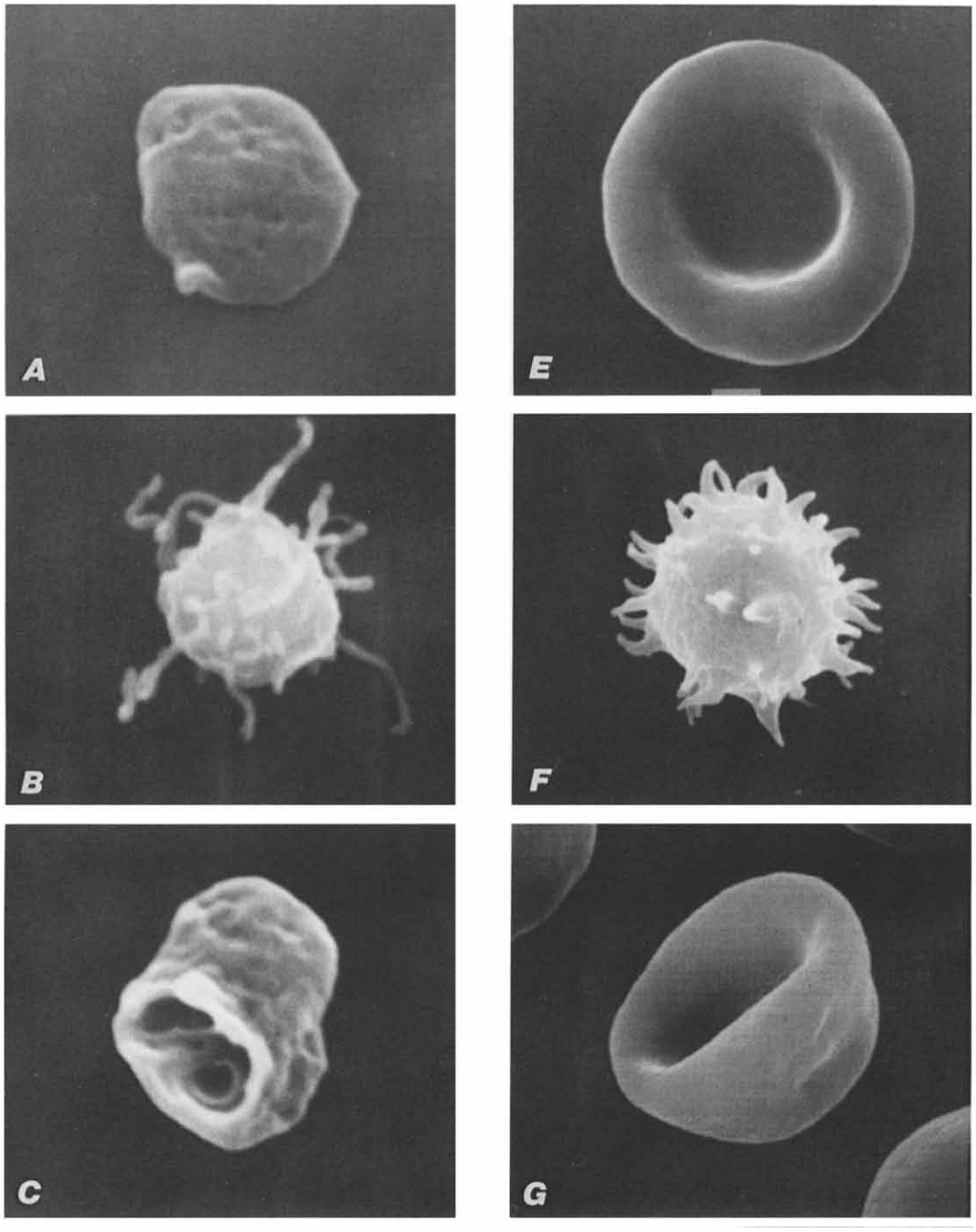

cAMP-phosphodiesterases are calmodulin-dependent, it seemed plausible that these compounds might reverse spiculation and cause sphering by raising intracellular cAMP. However, the phosphodiesterase inhibitors theophylline (3 mM) and 3-isobutyl-1-methylxanthine (IBMX, 900 μM) had no effect on platelet shape and did not alter the shape of platelets incubated with thrombin (1 U/ml), PAF (7 μM), or egg lysoPC (25 μM).

Cytochalasins bind to the rapidly growing end

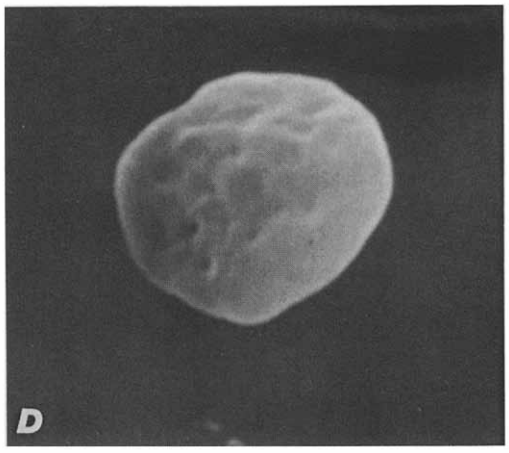

Fig. 4. Comparison of amphipath-treated erythrocytes and platelets. (A) Untreated platelet. (B) Spiculate platelet after incubation with egg lysoPC as in Figure 1B. (C) Indented platelet after incubation with chlorpromazine as in Fig. 1C. (D) Discoid platelet after incubation with egg lysoPC followed by chlorpromazine as in Fig. 1D. (E) Untreated erythrocyte. (F) Spiculate erythrocyte (echinocyte) after incubation with egg lysoPC (25 μM) at 10% hematocrit. (G) Indented erythrocyte (stomatocyte) after incubation with chlorpromazine (100 μM) at 10% hematocrit. Magnification: A–D, 20000×; E–G, 7000×.

of actin filaments and prevent addition of further monomers. They also inhibit thrombin-induce platelet shape changes [38,39]. However, cytochalasin E (1 μM) and colchicine (10 mM) had no effect on egg lysoPC-induced spiculation (Brunauer, L.S. and Mitchell, K.T., unpublished observations).

Amphipath-induced shape changes in erythrocytes

In general, zwitterionic and anionic amphipaths induce red cell crenation (Fig. 4F). As described previously [30], egg lysoPC, DLPC, and DMPC were potent crenators, inducing rapid echinocytosis at micromolar concentrations (Table I). The structurally similar compound PAF was about equally potent as a red cell crenator. This suggests that the compound acts on red cells simply as an outer monolayer intercalator, not through specific receptors as is the case in platelets. 1-Pyrenebutyric acid was a much less potent crenator (Table I), in agreement with a previous report [40]. Chlorotetracycline caused red cell crenation in the presence, but not the absence, of 1 mM extracellular calcium, in agreement with a previous report [41]. DLPS causes transient crenation followed by stomatocytosis [31]. The half-times for crenation varied from less than 30 s for egg lysoPC and fluorescein to 1.2 ± 0.3 min for DLPC and 70 ± 20 min for DMPC. Thrombin (1 U/ml) had no effect on red cell shape.

The cationic amphipaths chlorpromazine, dibucaine, and tetracaine caused red cells to cup and invaginate (Fig. 4G) as described previously

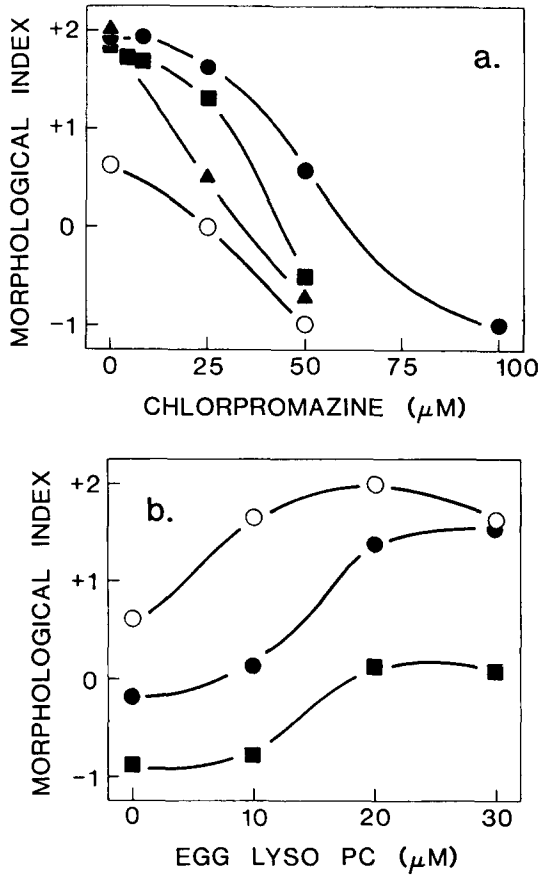

Fig. 5. Compensatory shape changes in platelets. (a) Platelets ($1.8 \cdot 10^8$/ml) were incubated for 5 min at 37°C with egg lysoPC (25 μM, ●), PAF (7 μM, ■), thrombin (1 U/ml, ▲), or no additive (○), then incubated for 10 min at 37°C with chlorpromazine at the concentrations shown. (b) Platelets ($1.7 \cdot 10^8$/ml) were incubated for 5 min with chlorpromazine (0, ○; 30 μM, ●; 60 μM, ■), then incubated 10 min with egg lysoPC at the concentrations shown.

[42]. This shape change was complete within 5 min. The cationic amphipaths also reversed the morphological effects of egg lysoPC, DLPC, DMPC, and metabolic crenation induced by ATP depletion.

Amphipath effects on lipid and protein phosphorylation

Platelets were labeled with $^{32}P_i$, washed, and incubated with DLPC (40 μM). Aliquots were assessed for cell morphology (Fig. 6), protein phosphorylation (Fig. 8), and lipid phosphorylation (Fig. 6). As shown in Fig. 8, DLPC treatment produced no changes in the labeling of myosin light chain 1 (MLC1), the 47 kDa kinase C substrate, or any of the other prominent phosphoprotein bands. In contrast, thrombin stimulation caused prominent labeling of both MLC1 and p47 within 20 s, and a slower increase in the labeling of one or two 24–26 kDa protein bands. The smaller of these co-migrates with a putative substrate of cAMP-dependent protein kinase (Ref. 37, and data not shown). A modest elevation in actin binding protein phosphorylation could be detected on 6% polyacrylamide gels following thrombin treatment, but not following DLPC treatment (not shown).

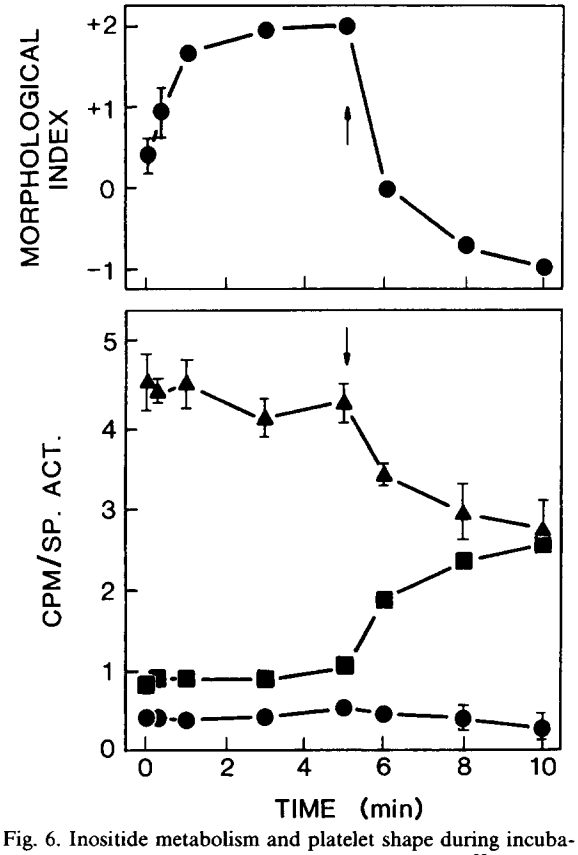

Fig. 6. Inositide metabolism and platelet shape during incubation with DLPC followed by chlorpromazine. ^{32}P-labeled platelets ($5 \cdot 10^8$/ml) were incubated with DLPC (40 μM) at 37 °C; aliquots were taken at the times shown. Chlorpromazine was added immediately following the 5 min time point, to yield a final concentration of 140 μM. Morphology (upper panel) and ^{32}P-labeling (lower panel) of PI (▲), PIP (■), and PIP_2 (●) were assessed. Inositide data are expressed as cpm/specific activity, where specific activity, measured in cpm/mol% phospholipid, was determined at $t = 0$. If the specific activity remained constant throughout the incubation, the radiolabel data also represent the relative masses of the inositides in mol%. Points represent mean ± S.E. for two separate experiments. Error bars are omitted where they are smaller than the plotted symbols.

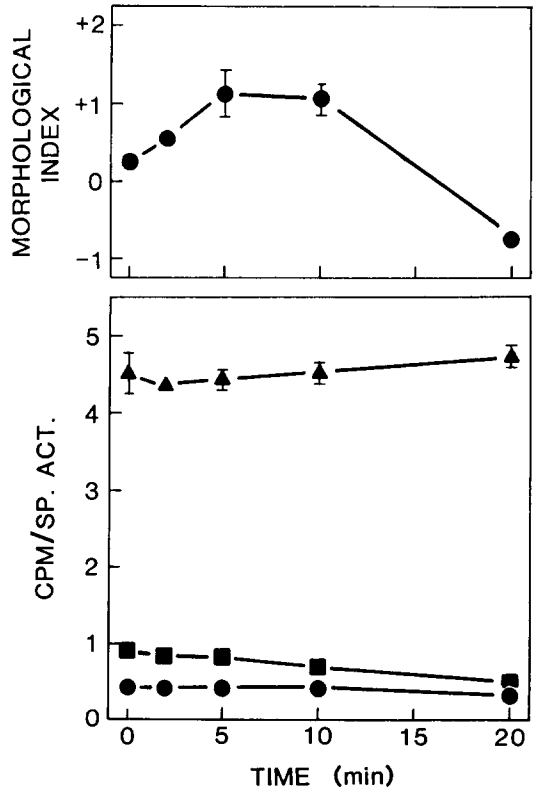

Fig. 7. Inositide metabolism and platelet shape during incubation with DLPS. ^{32}P-labeled platelets ($\cdot 10^8$/ml) were incubated with DLPS (50 μM). Morphology (upper panel) and inositide labeling (PI, ▲; PIP, ■; PIP_2, ●) were measured and are plotted as described for Fig. 6. Data shown are from two consecutive experiments using platelets from one batch of radiolabeled cells.

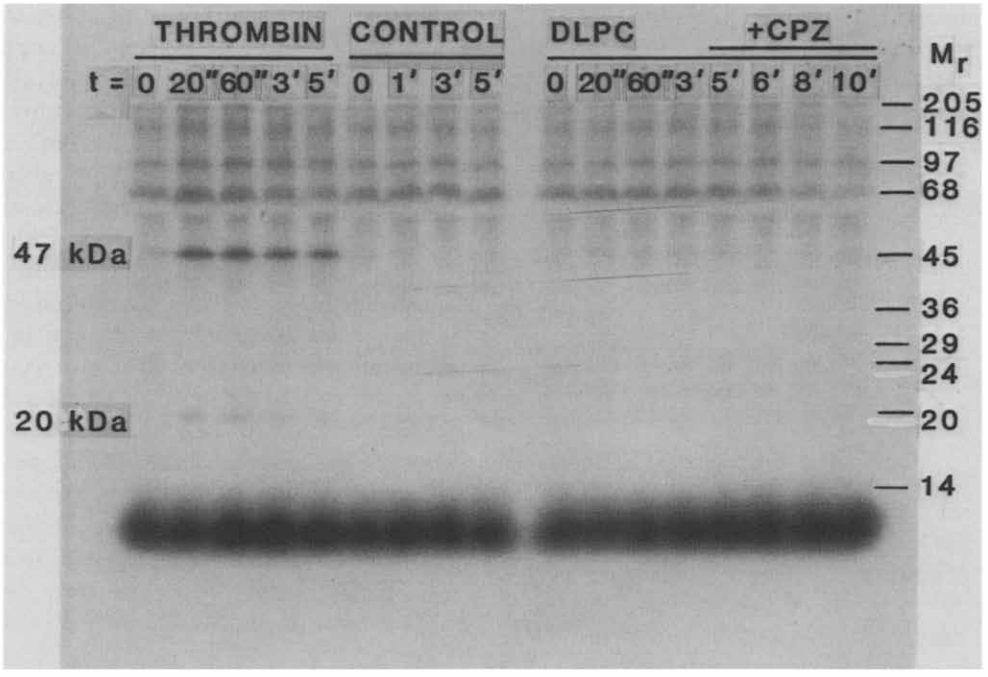

Fig. 8. Autoradiogram of platelet phosphoproteins during incubation with DLPC, chlorpromazine, and thrombin. ^{32}P-labeled platelets ($5 \cdot 10^8$ cells/ml) were incubated with thrombin (1 U/ml), no additive, or DLPC (40 μM) followed by chlorpromazine (140 μM). Samples were analyzed by SDS 12.5% polyacrylamide gel electrophoresis followed by autoradiography. Coomassie blue staining verified that equal amounts of protein were loaded in each lane. Molecular weight markers are shown on the right.

After 5 min incubation with DLPC, chlorpromazine was added to yield a final concentration of 140 μM. Over the next 5 min, chlorpromazine caused retraction (or loss) of filopodia, recovery of the discoid shape, and then sphering. These morphological changes were accompanied by two major changes in the phosphoprotein labeling pattern (Fig. 8). There was a small decrease in the labeling of most substrates, most prominently a 50% decrease in the labeling of a 70 kDa protein of unknown identity. These changes were not seen in platelets incubated with DLPC alone (not shown).

DLPC-induced spiculation was not accompanied by significant changes in phosphoinositide labeling (Fig. 6), nor were changes seen in PA or PC labeling (not shown). In contrast, thrombin-induced spiculation was accompanied by increasing labeling of PA and a transient decrease in [PIP_2] (not shown), as previously reported [43,44]. Upon chlorpromazine treatment, there was a 2.5- to 3-fold increase in PIP labeling accompanied by a decrease in PI labeling and possibily also a decrease in PIP_2 labeling. These changes were not seen in cells incubated with DLPC alone (not shown). The time courses for the lipid population changes and morphological changes were similar. No increase in PA labeling was seen (not shown). Under somewhat different incubation conditions (EDTA in the suspending medium and no DLPC treatment) chlorpromazine has been reported to increase both PIP and PIP_2 labeling [45].

In a similar experiment, platelets were prelabeled with [^{32}P]P_i, washed, and incubated with DLPS (50 μM). The cells first became spiculate, then discoid, and finally spheroid (Fig. 7). These shape changes were accompanied by no changes in the phosphorylation of MLC1, p47, or any other phosphoprotein bands. There were decreases in the labeling of PIP (50%) and PIP_2 (20%) detectable 10 to 20 min post-DLPS treatment. An increase (not statistically significant) in PI labeling was seen, possibly accounting for the decreases in PIP and PIP_2. No change in PA labeling was

detected (not shown).

As assessed by Coomassie blue staining of SDS-polyacrylamide gels, there were no changes in the gross platelet protein composition following DLPC, DLPS, or chlorpromazine treatment.

Discussion

Platelets incubated with various anionic and zwitterionic amphipaths develop fine filopodia. The discoid cell body becomes rounder, and the open canalicular system less prominent. These spiculate platelets resemble cells exposed to ADP, PAF, and other physiological platelet activators. Amphipath-induced spiculation is not accompanied by aggregation, nor are DLPC, DMPC, and DLPS-induced shape changes accompanied by serotonin release (Brunauer, L.S., unpublished results). Amphipath-induced spiculation occurs and persists in the presence of aspirin, albumin, cytochalasin E, apyrase, creatine phosphate/phosphocreatine kinase, theophylline, and IBMX.

Cationic amphipaths restore spiculate platelets to the discoid shape. The few spiculate platelets always found in untreated platelet suspensions become discoid when treated with low concentrations of such amphipaths, as do maximally spiculate thrombin-, PAF-, DLPC-, and egg lysoPC-treated platelets. Higher concentrations of cationic amphipaths cause platelets to become more nearly spherical and indented, and their canalicular systems possibly become more prominent. Occasionally such cells display large invaginations, possibly exaggerated entrances to the canalicular system. Zwitterionic amphipaths reverse chlorpromazine-induce cupping and restore platelets to apparently normal resting morphology *.

Possible mechanisms for amphipath-induced shape changes

It seemed plausible that amphipaths might exert their morphological effects by impinging upon activation-associated biochemical processes. However, after examining lipid and protein phosphorylation in platelets treated with DLPC, DLPS, and chlorpromazine, no such explanation is apparent. This is clearest in the case of DLPC. DLPC was found to induce spiculation without altering the phosphorylation of myosin light chain-1 or actin binding protein, both of which have been associated with shape changes induced by physiological activators [46,47]. DLPC caused no changes in inositide labeling, and no increase in the phosphorylation of the 47 kDa protein kinase C substrate. Thus DLPC appears to bypass the changes in platelet inositide metabolism and protein phosphorylation generally associated with platelet activation.

Two prominant biochemical changes of uncertain significance accompanied chlorpromazine-induced de-spiculation and sphering. First, there was a marked increase in PIP, largely at the expense of PI. Perhaps cationic amphipaths bind to the polyanionic PIP, shielding it from further metabolism. Aminoglycoside antibiotics like neomycin are thought to alter inositide metabolism by a similar mechanism [48]. Second, chlorpromazine caused loss of radiolabel from most of the phosphoproteins detected. This could be due to activation of a phosphatase with low specificity, or perhaps to changes in the specific activity of the intracellular metabolic ATP pool.

As previously noted [31], DLPS was found to cause transient spiculation followed by chlorpromazine-like sphering. The only biochemical change detected during these shape changes was a loss of radiolabel from PIP, and perhaps also PIP_2. This loss of PIP appeared to accompany the sphering phase of the DLPS-induced shape changes (although it is possible that a small decrease in PIP labeling accompanied the earlier spiculation phase as well). The observed change in lipid labeling contrasts with the chlorpromazine-induced increase in PIP and loss of PI. DLPS did not alter protein phosphorylation and no proteolysis was detected. Thus, the biochemical changes that accompany chlorpromazine-induced sphering are not seen during DLPS-induced sphering.

Bilayer balance and erythrocyte shape

Spiculate platelets bear a superficial structural

* Nachmias and co-workers have shown that local anesthetic-induced platelet sphering becomes irreversible at long times (1–2 h) or at high anesthetic concentrations [23]. This irreversibility (not the sphering per se) coincides with proteolysis of actin binding protein and talin. Under the conditions used in the present work, sphering was reversible (Fig. 5), and no proteolysis was noted on Coomassie blue stained electrophoretograms.

resemblance to crenated erythrocytes (echinocytes). Erythrocytes undergo morphological changes to yield spiculate echinocytes or indented, cupped stomatocytes in response to a variety of treatments, among them exposure to amphipaths. The prevailing explanation for the effects of amphipaths on erythrocyte shape is the 'bilayer couple' hypothesis [49]. This hypothesis asserts that cationic amphipaths concentrate in the membrane inner monolayer through energetically favorable interactions with acidic inner leaflet phospholipids; the resulting shape change, stomatocytosis, allows the membrane to geometrically accommodate the expanded inner leaflet. Zwitterionic and anionic amphiphaths concentrate in the outer leaflet through kinetic trapping and energetically unfavorable inner leaflet interactions, respectively, thereby expanding its relative area and causing echinocytosis. Exquisitely small changes in membrane bilayer balance (roughly 1% relative expansion of either leaflet) are sufficient for these shape changes [30,50,51]. Other processes (ATP depletion and calcium loading) also cause echinocytosis. It has been proposed that these shape changes also arise from changes in bilayer balance – inner monolayer shrinkage secondary to phosphoinositide catabolism [24–26]. Echinocytosis and stomatocytosis are in a sense opposite processes; stomatocytogenic compounds like chlorpromazine reverse the morphological effects of calcium loading, metabolic depletion, or echinocytogenic amphipaths.

This hypothesis remains controversial [52–54], and alternative hypotheses centered on the membrane skeleton as the driving force in echinocytosis/stomatocytosis have been advanced [55,56]. These alternatives have yet to be tested thoroughly.

Bilayer balance and platelet shape

Two observations suggest a connection between erythrocyte and platelet shape changes. First, there is some resemblance between the spiculate, discoid, and indented forms of each cell type (Fig. 4). Second, all echinocytic amphipaths tested induced platelet spiculation and all stomatocytogenic amphipaths caused platelet sphering (Table I). DLPS caused transient spiculation (echinocytosis) followed by sphering (stomatocytosis) in both cell types. Thus it is possible that platelet shape changes are governed by changes in bilayer balance. Whenever platelets are treated with agents that expand the plasma membrane outer monolayer relative to the inner monolayer, the cells become spiculate and the canalicular system less prominent. Expansion of the inner monolayer causes a loss of spicules and greater prominence of the canalicular system. These changes are shown schematically in Fig. 9.

The morphological effects of all of the amphipaths examined in this work are consistent with the bilayer balance hypothesis. We envision that egg lysoPC, DLPC, and DMPC transfer as monomers [36] to the platelet plasma membrane, intercalate in its outer monolayer, and remain kinetically trapped there for hours to days. DLPS likely transfers rapidly to the platelet outer monolayer and then translocates to the inner leaflet on a time scale of 10 to 20 min. This translocation may be mediated by a PS-specific 'flippase', an activity inferred from shape changes [31] and spin label studies [58] in platelets, and from a variety of approaches in erythrocytes [31,57]. 1-Pyrenebutyric acid and fluorescein likely partition between the membrane monolayers, favoring the outer leaflet. The partitioning of chlorotetracycline favors whichever side faces the higher calcium concentration. The cationic amphipaths may bind preferentially to the inner leaflet, or may expand the inner leaflet by promoting conversion of PI to the larger PIP. Though direct evidence of these proposed binding modes is lacking for platelets, a large body of work on erythrocytes and other

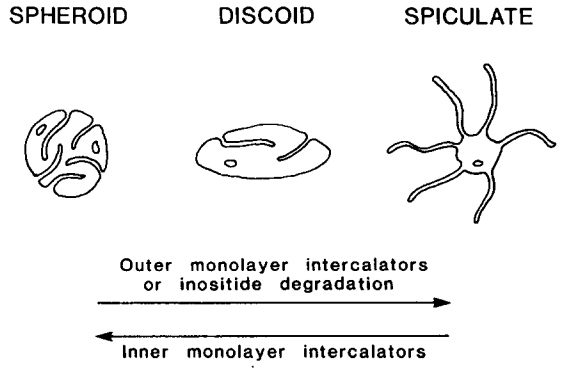

Fig. 9. Schematic view of the relationship between bilayer balance and platelet shape.

membrane systems supports their plausibility [30,31,36,40–42,49].

Elementary geometrical considerations show that the spiculate shape allows, in fact requires, expansion of the plasma membrane outer monolayer. The cell membrane can be divided into three contiguous domains: the cell body, with a nearly even balance of inner and outer monolayer surface areas for spherical, discoid, or even biconcave discoid shapes (outer/inner monolayer area ≈ 1.01); filopodia, which possess excess outer monolayer area (for a 100 nm filopodium with a 5 nm thick membrane, outer/inner monolayer area ≈ 1.10); and the canalicular system, with excess inner monolayer area (outer/inner monolayer area ≈ 0.90). Losing canalicular structures and/or gaining filopodia requires an increase in outer monolayer area; the reverse requires a decrease.

The bilayer balance hypothesis presupposes that the trans-bilayer distribution of platelet lipids remains more or less intact during amphipath-induced shape changes. It has been shown that this distribution is altered upon platelet stimulation by thrombin plus collagen; more phosphatidylserine becomes accessible to the extracellular phase for prothrombin conversion or phospholipase A_2 degradation [59]. Under some conditions, however, thrombin or collagen alone fail to induce PS exposure [59,60]. It remains to be seen whether amphipath treatment, a more limited form of 'activation' (shape change without aggregation or secretion), causes similar alterations.

It is unclear how the remodeling of the cytoskeleton that accompanies platelet shape changes [20] might regulate or be regulated by manipulations of the plasma membrane bilayer balance. This deficiency notwithstanding, we feel that the bilayer balance hypothesis provides a useful framework for understanding platelet shape. It accounts for the morphological effect of many amphipaths [22,23], successfully predicts the effects of other amphipaths (the present work), and provides a rationale for the common morphological effects of structurally dissimilar compounds.

The morphological effects of physiological activators like thrombin, collagen, and ADP might also involve bilayer balance changes. Wilson et al. [3] have estimated that thrombin-stimulated human platelets rapidly lose about 10 nmol PI per 10^9 cells, or about $6 \cdot 10^6$ molecules/cell. Conversion of PI to diacylglycerol and phosphatidic acid should shrink the membrane inner monolayer and thereby upset the bilayer balance. A comparable change in bilayer balance might be expected to result from the insertion into the membrane outer monolayer of $6 \cdot 10^6$ molecules of exogenous DLPC per cell, which, as shown above, is sufficient to cause marked spiculation. Thus, inositide hydrolysis may serve not only to generate crucial second messengers, but also to alter the preferred contour of the plasma membrane through changes in bilayer balance. If so, this might explain how thrombin and PAF can cause spiculation under conditions where they do not elevate intracellular calcium [13,15].

Acknowledgements

We thank Dr. Linda S. Brunauer for advice and assistance on platelet isolation, Dr. David L. Daleke for generously providing the DLPS used herein, and Frances C. Thomas for carrying out the transmission electron microscopy. This work was supported by grants from the National Institutes of Health (HL 23787 and Syntex Research, Division of Syntex (U.S.A.), Inc.

References

1 Zucker, M.B. and Nachmias, V.T. (1985) Arteriosclerosis 5, 2–18.
2 Rink, T.J. and Hallam, T.J. (1984) Trends Biochem. Sci. 9, 215–219.
3 Wilson, D.B., Neufeld, E.J. and Majerus, P.W. (1985) J. Biol. Chem. 260, 1046–1051.
4 Berridge, M.J. (1984) Biochem. J. 220, 345–360.
5 Majerus, P.W., Connolly, T.M., Deckmyn, H., Ross, T.S., Bross, T.E., Ishii, H., Bansal, V.S. and Wilson, D.B. (1986) Science 234, 1519–1526.
6 Wilson, D.B., Connolly, T.M., Bross, T.E., Majerus, P.W., Sherman, W.R., Tyler, A.N., Rubin, L.J. and Brown, J.E. (1985) J. Biol. Chem. 260, 13496–13501.
7 Nishizuka, Y. (1984) Nature (Lond.) 308, 693–698.
8 Hathaway, D.R. and Adelstein, R.J. (1979) Proc. Natl. Acad. Sci. USA 76, 1653–1657.
9 Billah, M.M., Lapetina, E.C. and Cuatrecasas, P. (1980) J. Biol. Chem. 255, 10227–10231.
10 Fox, J.E.B., Reynolds, C.C. and Phillips, D.R. (1983) J. Biol. Chem. 258, 9973–9981.
11 Connolly, T.M., Lawing, W.J., Jr. and Majerus, P.W. (1986) Cell 46, 951–958.

12 Touqui, L., Rothhut, B., Shaw, A.M., Fradin, A., Vargaftig, B.B. and Russo-Marie, R. (1986) Nature (Lond.) 321, 177–180.
13 Rink, T.J., Smith, S.W. and Tsien, R.Y. (1982) FEBS Lett. 148, 21–26.
14 Kaibuchi, K., Takai, Y., Sawamura, M., Hoshijima, M., Fujikura, T. and Nishizuka, Y. (1983) J. Biol. Chem. 258, 6701–6704.
15 Hallam, T.J., Sanchez, A. and Rink, T.J. (1984) Biochem. J. 218, 819–827.
16 Lapetina, E.G., Silio, J. and Ruggiero, M. (1985) J. Biol. Chem. 260, 7078 ± 7083.
17 White, J.G., Rao, G.H.R. and Estensen, R.D. (1974) Am. J. Pathol. 75, 301–314.
18 Rink, T.J., Sanchez, A. and Hallam, T.J. (1983) Nature (Lond.) 305, 317–319.
19 Reimers, H.J., Packham, M.A., Kinlough-Rathbone, R.L. and Mustard, J.F. (1973) Br. J. Haematol. 25, 675–689.
20 Nachmias, V.T. (1983) Semin. Hematol. 20, 261–281.
21 Jennings, L.K., Fox, J.E.B., Edwards, H.H. and Phillips, D.R. (1981) J. Biol. Chem. 256, 6927–6932.
22 Kanaho, Y. and Fujii, T. (1982) Biochem. Biophys. Res. Commun. 106, 513–519.
23 Nachmias, V.T., Sullender, J.S. and Fallon, J.R. (1979) Blood 53, 63–72.
24 Ferrell, J.E., Jr. and Huestis, W.H. (1985) J. Cell Biol. 98, 1992–1998.
25 Allan, D. and Michell, R.H. (1975) Nature (Lond.) 258, 348–349.
26 Allan, D. and Thomas, P. (1981) Biochem. J. 198, 433–440.
27 Tangen, O. and Berman, H.J. (1972) Adv. Exp. Med. Biol. 34, 235–243.
28 Vigo, C. (1985) J. Biol. Chem. 260, 3418–3422.
29 Comfurius, P. and Zwaal, R.F.A. (1977) Biochim. Biophys. Acta 488, 36–42.
30 Ferrell, J.E., Jr., Lee, K.-J. and Huestis, W.H. (1985) Biochemistry 24, 2849–2857.
31 Daleke, D.L. and Huestis, W.H. (1985) Biochemistry 24, 5406–5416.
32 Broekman, M.J., Ward, J.W. and Marcus, A.J. (1980) J. Clin. Invest. 66, 275–283.
33 Laemmli, U.K. (1970) Nature (Lond.) 227, 680–685.
34 White, J.G. (1984) in Blood Platelet Function and Medicinal Chemistry (Lasslo, A., ed.), pp. 15–59, Elsevier Biomedical, New York.
35 Kobayashi, T., Okamoto, H., Yamada, J.-I., Setaka, M. and Kwan, T. (1984) Biochim. Biophys. Acta 778, 210–218.
36 Ferrell, J.E., Lee, K.-J. and Huestis, W.H. (1985) Biochemistry 24, 2857–2864.
37 Haslam, R.J., Davidson, M.M.L., Davies, T., Lynham, J.A. and McClenaghan, M.D. (1978) Adv. Cyclic Nucleotide Res. 9, 533–552.
38 Fox, J.E.B. and Phillips, D.R. (1981) Nature (Lond.) 292, 650–652.
39 Casella, J.F., Flanagan, M.D. and Lin, S. (1981) Nature (Lond.) 293, 302–305.
40 Matayoshi, E.D. (1980) Biochemistry 19, 3414–3422.
41 Riquelme, G., Jaimovich, E., Lingsch, C. and Behn, C. (1982) Biochim. Biophys. Acta 689, 219–229.
42 Fuji, T., Sato, T., Tamura, A., Wakatsuki, M. and Kanaho, Y. (1979) Biochem. Pharmacol. 28, 613–620.
43 Agranoff, B.W., Murthy, P. and Seguin, E.B. (1983) J. Biol. Chem. 258, 2076–2078.
44 Billah, M.M. and Lapetina, E.G. (1982) J. Biol. Chem. 257, 12705–12708.
45 Tallant, E.A. and Wallace, R.W. (1985) Biochem. Biophys. Res. Commun. 131, 370–377.
46 Daniel, J.L., Molish, I.R., Rigmaiden, M. and Stewart, G. (1984) J. Biol. Chem. 259, 9826–9831.
47 Carroll, R.C. and Gerrard, J.M. (1982) Blood 59, 466–471.
48 Schacht, J. (1976) J. Neurochem. 27, 1119–1124.
49 Sheetz, M.P. and Singer, S.J. (1974) Proc. Natl. Acad. Sci. USA 71, 4457–4461.
50 Beck, J.S. (1978) J. Theor. Biol. 75, 487–501.
51 Lange, Y. and Slayton, J. (1982) J. Lipid Res. 23, 1121–1127.
52 Conrad, M.J. and Singer, S.J. (1981) Biochemistry 20, 808–818.
53 Chalpin, D.B. and Kleinfeld, A.M. (1983) Biochim. Biophys. Acta 731, 465–474.
54 Liever, M.R., Lange, Y., Weinstein, R.S. and Steck, T.L. (1984) J. Biol. Chem. 259, 9225–9234.
55 Anderson, R.A. and Marchesi, V.T. (1985) Nature (Lond.) 318, 295–298.
56 Jinbu, Y., Sato, S. and Nakao, M. (1984) Nature (Lond.) 307, 376–378.
57 Seigneuret, M. and Devaux, P.F. (1984) Proc. Natl. Acad. Sci. USA 81, 3751–3755.
58 Sune, A., Bette-Bobillo, P., Bienvenue, A., Fellmann, P. and Devaux, P.F. (1987) Biochemistry 26, 2972–2978.
59 Bevers, E.M., Comfurius, P., Van Rijn, J.L.M.L., Hemker, H.C. and Zwaal, R.F.A. (1982) Eur. J. Biochem. 122, 429–436.
60 Bevers, E.M., Confurius, P. and Zwaal, R.F.A. (1983) Biochim. Biophys. Acta 736, 57–66.